synthase and acyltransferase active site motifs in a type II polyketide synthase of *Streptomyces glaucescens*. *J. Bacteriol.* **177,** 477–481 (1995).
20. Joshi, A. K., Witkowski, A. & Smith, S. Mapping of functional interactions between domains of the animal fatty acid synthase by mutant complementation *in vitro*. *Biochemistry* **36,** 2316–2322 (1997).
21. Wiesmann, K. E. H. *et al*. Polyketide synthesis *in vitro* on a modular polyketide synthase. *Chem. Biol.* **2,** 583–589 (1995).
22. Pieper, R., Luo, G. L., Cane, D. E. & Khosla, C. Remarkably broad substrate specificity of a modular polyketide synthase in a cell-free system. *J. Am. Chem. Soc.* **117,** 11373–11374 (1995).
23. Kao, C. M., Pieper, R., Cane, D. E. & Khosla, C. Evidence for two catalytically independent clusters of active sites in a functional modular polyketide synthase. *Biochemistry* **35,** 12363–12368 (1996).
24. Weissman, K. J., Bycroft, M., Staunton, J. & Leadlay, P. F. Origin of starter units for erythromycin biosynthesis. *Biochemistry* **37,** 11012–11017 (1998).
25. Marsden, A. F. A. *et al*. Engineering broader specificity into an antibiotic-producing polyketide synthase. *Science* **279,** 199–202 (1998).
26. Rowe, C. J., Cortés, J., Gaisser, S., Staunton, J. & Leadlay, P. F. Construction of new vectors for high-level expression in actinomycetes. *Gene* **216,** 215–223 (1998).
27. Crosby, J. *et al*. Polyketide synthase acyl carrier proteins from *Streptomyces*: expression in *Escherichia coli*, purification and partial characterization. *Biochim. Biophys. Acta* **1251,** 32–42 (1995).

Acknowledgements

This work was supported by grants from the BBSRC (UK) (to J.S. and P.F.L., and to T.J.S.), from the EPSRC (UK) (studentship to J.W.), from the Swiss National Science Foundation (to C.B.) and from Pfizer Inc. We thank H. A. I. McArthur, M. Oliynyk and C. J. Wilkinson for helpful advice.

Correspondence and requests for materials should be addressed to P.F.L. (e-mail: pfl10@mole.bio.cam.ac.uk).

Myosin VI is an actin-based motor that moves backwards

Amber L. Wells*, Abel W. Lin†, Li-Qiong Chen*, Daniel Safer*, Shane M. Cain‡, Tama Hasson‡, Bridget O. Carragher§, Ronald A. Milligan† & H. Lee Sweeney*

* *Department of Physiology, University of Pennsylvania School of Medicine, 3700 Hamilton Walk, Philadelphia, Pennsylvania 19104-6085, USA*
† *Department of Cell Biology, The Scripps Research Institute, 10550 North Torrey Pines Road, La Jolla, California 92037, USA*
‡ *Department of Biology, University of California, San Diego, La Jolla, California 92093-0368, USA*
§ *Beckman Institute, Dept. of Cell and Structural Biology, University of Illinois at Urbana-Champaign, Urbana, Illinois 61801, USA*

Myosins and kinesins are molecular motors that hydrolyse ATP to track along actin filaments and microtubules, respectively. Although the kinesin family includes motors that move towards either the plus or minus ends of microtubules[1], all characterized myosin motors move towards the barbed (+) end of actin filaments[2]. Crystal structures of myosin II (refs 3–6) have shown that small movements within the myosin motor core are transmitted through the 'converter domain' to a 'lever arm' consisting of a light-chain-binding helix and associated light chains[5,6]. The lever arm further amplifies the motions of the converter domain into large directed movements[3,5–7]. Here we report that myosin VI, an unconventional myosin[8–12], moves towards the pointed (−) end of actin. We visualized the myosin VI construct bound to actin using cryo-electron microscopy and image analysis, and found that an ADP-mediated conformational change in the domain distal to the motor, a structure likely to be the effective lever arm, is in the opposite direction to that observed for other myosins. Thus, it appears that myosin VI achieves reverse-direction movement by rotating its lever arm in the opposite direction to conventional myosin lever arm movement.

Although all myosin motors so far characterized move towards the barbed (+) end of actin filaments, there may well be cellular roles for oppositely directed myosins, and there are many unconventional myosins that have unknown functions and unusual primary structures[2,8]. The simplest way to reverse the direction of movement would be to keep the basic motor with both its actin interface and core nearly identical to other myosins, but to attach the lever arm in such a way that the same movements of the motor core would rotate the lever arm in the opposite direction on actin, as compared with other myosins. We therefore compared the sequences of all known myosins, looking for large differences beginning in the converter domain and ending at the first light-chain-binding motif. Of the 15 known classes of myosins, the members of the myosin VI class were the only ones that fulfilled this criterion. They contain a 53-amino-acid insertion in the converter/lever arm region (Fig. 1); therefore, myosin VI was the best candidate for a reverse-direction myosin.

Class VI myosins were first identified in *Drosophila melanogaster*[9] and were subsequently found to be expressed in species from *Caenorhabditis elegans* to human[8,10–12]. Myosin VI has a single

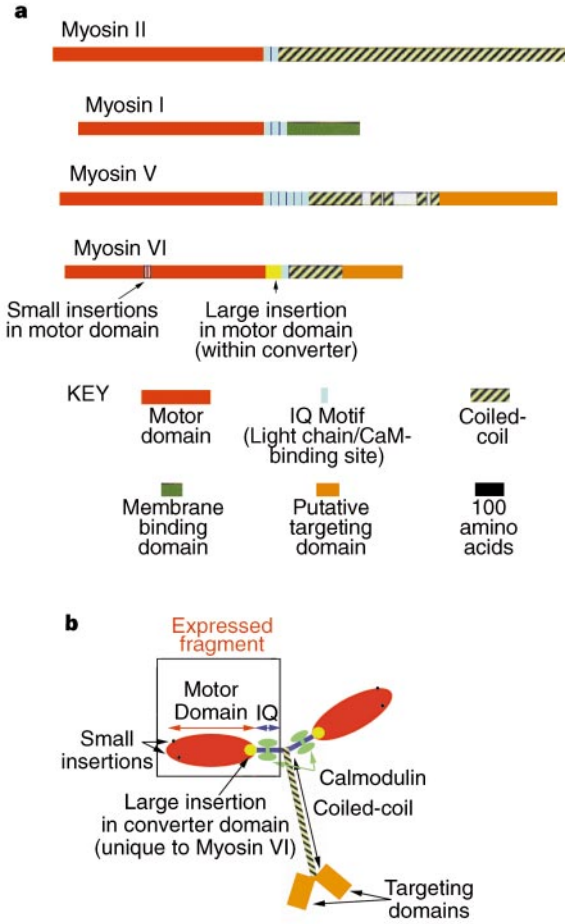

Figure 1 Myosin VI. **a**, Comparison of the primary structures of four classes of myosins. Two small insertions and one large insertion at the end of the motor domain (within the converter) comprise the main differences between the motor domain of myosin VI and those of other members of the myosin family. Conventional myosin (myosin II from smooth muscle) and two unconventional myosins (brush border myosin I and myosin V) all move toward the barbed (+) ends of actin filaments. There are differing numbers of light-chain/CaM-binding sites (IQ motifs) among these classes, as well as highly divergent C-terminal regions (to the right of the IQ motifs). **b**, The native myosin VI molecule, with a box around the truncation used in this study. The expressed fragment had additional amino acids after the IQ motif (C terminus) for purification and motility measurements (see Methods).

calmodulin (CaM)-binding site following the motor domain and contains a coiled-coil region as well as globular carboxy-terminal tail[2,8,10]. Myosin VI is found in a variety of cell types[13–15]. The myosin VI gene (*myo6*) is defective in the deaf mouse, Snell's waltzer[11], indicating that myosin VI may be required for the function of sensory hair cells[11,13]. Immunolocalization studies suggest that, in a variety of cell types, myosin VI is involved in vesicular transport[13,15].

We co-expressed CaM with a single-headed pig myosin VI construct coding for the region including the motor domain and the helical CaM-binding domain ('IQ' motif[8]) in insect SF9 cells (Fig. 1b). The purified protein had a single CaM bound per heavy chain. At 25 °C, the expressed myosin displayed maximal actin-activated ATPase activity of 0.8 per head s^{-1} ($K_{ATPase} = 3\ \mu M$), and moved actin filaments at an average velocity of $58 \pm 10\ nm\ s^{-1}$.

To determine definitively the direction of movement, we modified the standard *in vitro* motility assay[16] to create actin filaments with labelled pointed ends by polymerizing off the barbed end of rhodamine-labelled, cross-linked F-actin nuclei. We then stabilized the filaments with fluorescein isothiocyanate (FITC)-phalloidin. The resulting actin filaments were green throughout, with a red cap at the pointed end. These filaments confirmed that myosin V, like myosin I and myosin II, moves towards the barbed (+) end of actin filaments[17]. As shown in Fig. 2a, a surface-bound, truncated myosin V moved actin filaments so that the pointed end was at the front of the moving filament (that is, the myosin moved away from the pointed end, towards the barbed end). When filaments from the same preparation were put on myosin VI-coated surfaces, they moved in the opposite direction, showing that myosin VI moves toward the pointed (–) ends of the filaments (Fig. 2b). Data for a number of polarity-marked filaments are summarized in Fig. 2c), with positive velocity indicating movement toward the barbed (+) end and negative velocity indicating movement toward the pointed (–) end of an actin filament. All data confirm that myosin VI moves in the opposite direction to that of previously studied myosins.

We decorated actin filaments with our myosin VI construct for analysis by cryo-electron microscopy and image reconstruction to gain structural insight into the reverse-direction motility of myosin VI. We calculated three-dimensional maps of the truncated myosin VI bound to actin filaments in the presence and absence of ADP (Fig. 3a, b); these reveal that this myosin has an unusual shape.

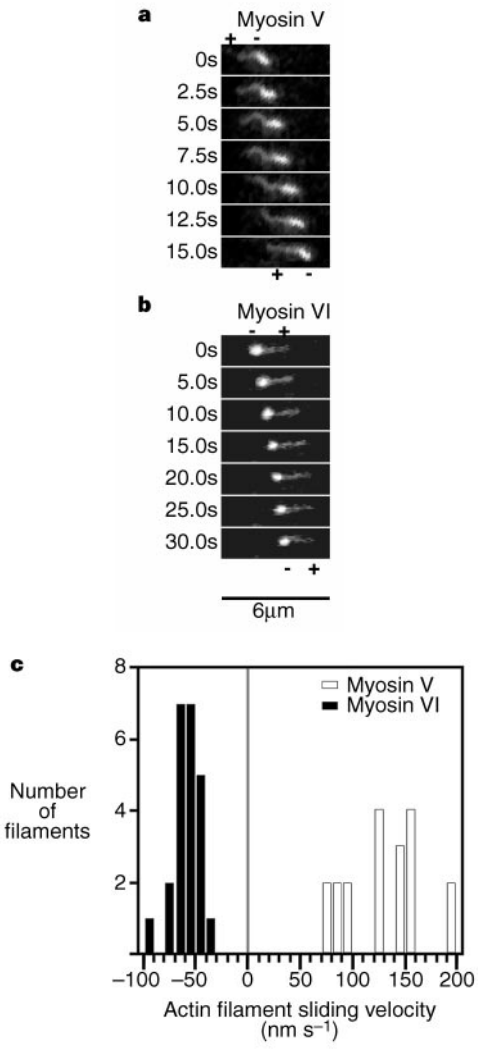

Figure 2 Determination of direction of myosin movement. Panels display the same spatial field at the relative times shown on the left. Within each panel is a single actin filament (visualized using FITC-phalloidin) moving in a conventional *in vitro* motility assay[17]. The bright (rhodamine/FITC-labelled) tip on each filament marks the pointed (–) end of the filament. **a**, Movement of actin by a myosin V construct containing the motor domain and one CaM/light-chain-binding site. The actin filament moves with the pointed (–) end leading, indicating that the myosin V moves towards the barbed (+) end. The filament sliding velocity was $140\ nm\ s^{-1}$ (25 °C). **b**, Movement of actin by a myosin VI construct containing the motor domain and its one CaM-binding site. The actin filament moves with the pointed (–) end trailing, indicating that the myosin VI moves toward the pointed (–) end. The filament sliding velocity was $60\ nm\ s^{-1}$ (25 °C). **c**, Histogram of the velocities of polarity-marked actin filaments moving on either myosin V or myosin VI. Movement of myosin towards the barbed (+) end was arbitrarily defined as positive velocity and movement toward the pointed (–) end as negative velocity.

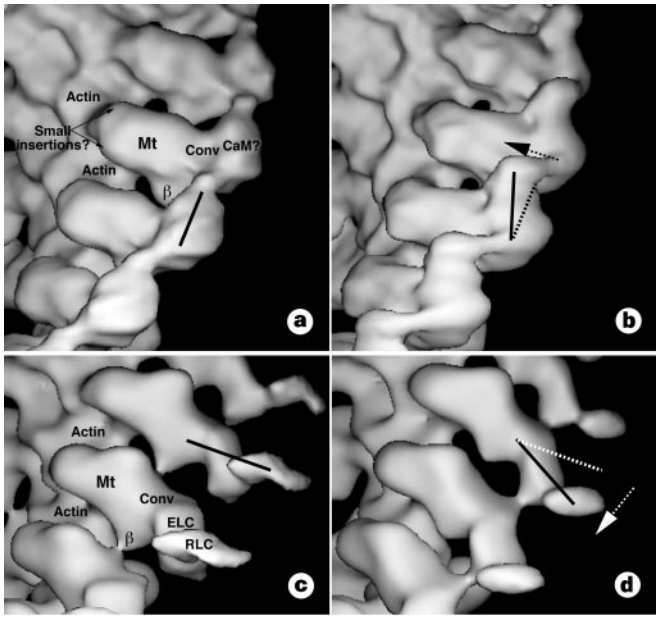

Figure 3 Comparison of ADP (left) and rigor (right) 3D maps of myosin VI (**a**, **b**), and smooth muscle myosin II (**c**, **d**) attached to F-actin. All maps are at the same scale; the vertical extent of the maps in **a** and **b** is ~250 Å. Solid lines indicate the long axes of the CaM- or light-chain-binding domains of the two myosins. Arrows show the direction of rotation of the domains in the transition between the ADP and rigor states. The data in **c** and **d** is taken from ref. 7. The rotation was roughly 15–20° for myosin VI, and 20–25° for myosin II. β denotes N-terminal β-barrel domains; Mt overlays the approximate positions of the cores of the myosin motors. Small Insertions? highlights regions of density found only in myosin VI which are the possible locations of the 9-amino-acid (lower arrow) and 13-amino-acid (upper arrow) inserts between the motor core and actin interface. Conv denotes the approximate locations of the converter domains. CaM? denotes the probable CaM density within myosin VI. ELC denotes the essential light chain and RLC the regulatory light chain of myosin II, which together constitute the effective lever arm.

Fig. 3a shows our single-headed myosin VI in the presence of 5 mM Mg-ADP. The myosin VI motor domain has the same geometry of attachment to F-actin as conventional myosin (Fig. 3c), but it has a number of differences that most probably reflect small differences in the primary structure. For example, myosin VI contains two small insertions of roughly 9 and 13 amino acids in a region between the nucleotide pocket and the actin-binding interface (insertions beginning at positions corresponding to residue 317 or 343 of the chicken skeletal myosin II sequence; see Figs 1 and 3a). The insertion of 53 amino acids, which is nominally between the converter domain and light-chain-binding helix, may in fact be a component of a radically divergent myosin VI converter domain. Indeed, the most notable differences between this map and maps of other myosins (myosin I, myosin II or myosin V) are in the light-chain-binding region, which has an unusual shape and orientation. At the resolution of this study, the location of the additional 53-amino-acid insert is unclear. Likewise, the CaM light chain is not unambiguously resolved, but we tentatively assign CaM to the region with an elongated, asymmetric shape (Fig. 3a).

We determined the unusual functional aspect of the structure by comparing nucleotide-bound (ADP) and nucleotide-free (rigor) states of the motor. For some isoforms of either myosin II (ref. 7) or myosin I (ref. 18), a part of the myosin conformational change on actin is associated with ADP dissociation. Thus, a comparison of the ADP and rigor structures of our myosin VI isoform on actin could show this movement, together with the structural features that move and the direction of the movement. Unlike other myosins in which the effective lever arm (light-chain-binding domain) projects out at a right angle to the filament axis (for example, brush border myosin I (ref. 18)) or towards the barbed end of the filament (for example, myosin II (ref. 7); Fig. 3c, d), the myosin VI lever arm (the putative CaM-binding domain) appears to project towards the pointed end of the actin filament (Fig. 3a, b). Furthermore, comparing the maps of ADP and rigor structures (Fig. 3a, b), shows that the lever arm clearly rotates in the opposite direction to myosin II when ADP is released from the head (Fig. 3c, d). Although little of the rotation associated with ADP release appears to be parallel to the actin filament, we hypothesize that the ADP-induced rotation observed is simply the final small fraction of the overall rotation associated with the myosin VI powerstroke; as is the case with smooth muscle myosin II (refs 5, 7).

Achieving reversal of myosin direction on actin by altering the converter domain/lever arm is analogous to the recently proposed strategy underlying direction determination within the kinesin motor family[19–21]. Directionality within the kinesin family is primarily a function of the neck region of the kinesin/ncd motors, with possible contributions from the stalk and, to a lesser extent, the motor core[21]. The neck and stalk elements must be involved in the different positioning of the second head of kinesin compared to ncd that is observed in cryo-electron microscopy reconstructions[20–23]. Although it is not clear that either of these kinesin structural elements functions as a true lever arm, the kinesin neck may be functionally analogous to the converter domain of myosin. Thus, the myosins and kinesins appear to use a similar general strategy to achieve reversal of movement. In each family, the motor core is preserved and direction of movement depends on how the same nucleotide-mediated movements are subsequently interpreted and amplified by other regions of the molecule.

Myosin VI has evolved to provide reverse-direction movement (that is, towards the pointed (−) end) on an actin filament. Sequence alignments indicate that it may be the only myosin class with a strategy of altering the converter domain, and thus may be unique among myosins in its direction of movement. This motor represents a means of providing (in conjunction with other classes of myosins) bidirectional movement on polarized actin filaments or filament bundles. A full understanding of the cellular importance of this motor awaits further investigation. □

Methods

Protein engineering and preparation

Myosin VI was expressed using the baculovirus/SF9 cell expression system. The expression and purification were as described[24]. To create the recombinant virus used for expression, we constructed a single-headed myosin VI by truncating the complementary DNA coding for pig myosin VI (ref. 10) after the codon corresponding to Gly 840. This construct encompassed the motor domain and the one CaM-binding site of myosin VI. Either a 'Flag' tag DNA sequence (encoding GDYKDDDDK)[25] or sequential '*myc*' (encoding EQKLISEEDL)[26] and Flag tags were appended to the truncated myosin VI coding sequence. A stop codon followed the Flag tag in both cases. We used the Flag tag for purification, and the Myc tag in *in vitro* motility assays to couple the myosin to nitrocellulose surfaces using an antibody against the Myc epitope. A full-length cDNA for chicken CaM was co-expressed with the truncated myosin VI heavy chain. The recombinant, truncated chicken myosin V (ref. 27) used in the motility experiments summarized in Fig. 2 was produced in the same manner. It was truncated after its first CaM/light-chain-binding site, at Arg 792. Both Myc and Flag tags were appended for motility assays and purification, respectively.

Functional assays

Determination of actin-activated ATPase activity (at 25 °C in 20 mM KCl) followed published procedures[24,28], as did the determinations (at 25 °C in 50 mM KCl) of actin-filament sliding velocity[16,24]. To use the *in vitro* motility assay to determine direction, actin filaments were generated that had red (rhodamine) labels at their pointed (−) ends. This involved the preparation of crosslinked, fluorescent actin nuclei by first dialysing 125 μM F-actin into 0.1 M KCl, 2.5 mM $Na_2B_4O_7$, 1 mM $MgCl_2$, 0.2 mM ATP, pH 9.0. Next, 1 mol *p*-phenylenedimaleimide (as a 10 mM solution in dimethylformamide (DMF)) was added per mol actin monomer, and crosslinking proceeded for 1 h at 25 °C (ref. 29). A fourfold excess of tetramethylrhodamine isothiocyanate was added (as a 33 mM solution in DMF), and the labelling reaction carried out for 2 h in the dark at 4 °C. The material was dialysed in the dark for 16 h against 5 mM Tris-HCl, 0.2 mM ATP, 0.2 mM $CaCl_2$, 0.2 mM NaN_3, pH 7.5, and then centrifuged for 30 min at 200,000 *g*, yielding a soluble supernatant and a depolymerization-resistant pellet of fluorescent F-actin. After the supernatant was polymerized by salt, pelleted, and redialysed against depolymerizing buffer, we obtained a second depolymerization-resistant pellet. The depolymerization-resistant pellets, which were highly enriched in actin dimers and higher oligomers as shown by SDS–PAGE, were used for rhodamine-labelled actin nuclei. The resuspended pellets were sheared through a 25-gauge needle to produce short filaments, and precipitated free dye was removed by centrifugation at 16,000*g* for 15 min. We added unlabelled actin to these nuclei at two different concentrations below the critical concentration for polymerization from the pointed end, but above the critical concentration for the barbed end (0.10 or 0.25 μM). Polymerization took place overnight. Filaments were stabilized by the addition of FITC-phalloidin, and inspection confirmed that a small percentage of the resulting FITC-labelled actin filaments contained a rhodamine tip (breakage of filaments probably creates many unlabelled nuclei for polymerization). The tip was visible in the rhodamine channel of a fluorescence microscope equipped with an intensified CCD camera. The entire filament was visible in the FITC channel. With dual excitation of rhodamine and FITC, the tip was brighter than the rest of the filament (Fig. 2), as it contained multiple rhodamine labels per actin monomer as well as FITC-phalloidin.

Electron microscopy and image analysis

Recombinant myosin VI at 2–5 mg ml^{-1} in 10 mM imidazole, pH 7.0, 50 mM KCl, 2 mM $MgCl_2$, 0.5 mM EDTA, 0.1 mM EGTA, 0.5 mM DTT was used to decorate platelet actin filaments adsorbed to holey carbon support films on electron microscopy grids. For the nucleotide-free condition, apyrase was added to the solution (final concentration ~10 U ml^{-1}) on the grid just before blotting and freezing in liquid ethane slush. For the ADP condition, the myosin buffer was supplemented with 5 mM Mg-ADP. We used a Gatan cold stage, operating at −180 °C, to examine the grids in a Philips CM200 FEG electron microscope. Images of filaments spanning holes in the support film were recorded at 40,000× at 1.1–2.0 μm under focus. Selected images of well ordered filaments were digitized with spot and step sizes equivalent at 4.97 Å at the specimen. Image analysis, averaging and calculation of 3D maps were carried out essentially as described[30]. Data from 43 (8,586 subunits) and 27 filaments (4,617 subunits) were averaged for the ADP and rigor structures, respectively. The resolution of the two final maps is 20–25 Å as judged from phase agreement along the layer lines. A full description of the data will be published elsewhere. The 3D maps were visualized with Volvis.

Received 24 June; accepted 12 August 1999.

1. Bloom, G. S. & Endow, S. A. Motor proteins 1: kinesins. *Protein Profile* **2,** 1105–1171 (1995).
2. Sellers, J. R. & Goodson, H. V. Motor proteins 2: myosin. *Protein Profile* **2,** 1323–1423 (1995).
3. Rayment, I. *et al.* Three-dimensional structure of myosin subfragment-1: A molecular motor. *Science* **261,** 50–58 (1993).
4. Fisher, A. J. *et al.* X-ray structures of the myosin motor domain of *Dictyostelium discoideum* complexed with MgADP.BeF_x and MgADP.AlF_4^-. *Biochem.* **34,** 8960–8972 (1995).
5. Dominguez, R., Freyzon, Y., Trybus, K. M. & Cohen, C. Crystal structure of a vertebrate smooth muscle myosin motor domain and its complex with the essential light chain: visualization of the pre-power stroke state. *Cell* **94,** 559–571 (1998).
6. Houdusse, A., Kalabokis, V. N., Himmel, D., Szent-Gyorgyi, A. G. & Cohen, C. Atomic structure of scallop myosin subfragment S1 complexed with MgADP: a novel conformation of the myosin head. *Cell* **97,** 459–470 (1999).

7. Whittaker, M. *et al.* A 35 Å movement of smooth muscle myosin on ADP release. *Nature* **378,** 748–751 (1995).
8. Mooseker, M. S. & Cheney, R. E. Unconventional myosins. *Annu. Rev. Cell Dev. Biol.* **11,** 633–675 (1995).
9. Kellerman, K. A. & Miller, K. G. An unconventional myosin heavy chain gene from *Drosophila melanogaster*. *J. Cell Biol.* **119,** 823–834 (1992).
10. Hasson, T. & Mooseker, M. S. Porcine myosin VI: characterization of a new mammalian unconventional myosin. *J. Cell Biol.* **127,** 425–440 (1994).
11. Avraham, K. B. *et al.* The mouse Snell's waltzer deafness gene encodes an unconventional myosin required for structural integrity of inner ear hair cells. *Nature Genet.* **11,** 369–375 (1995).
12. Avraham, K. B. *et al.* Characterization of human unconventional myosin-VI, a gene responsible for deafness in Snell's waltzer mice. *Hum. Mol. Genet.* **6,** 1225–1231 (1997).
13. Hasson, T. *et al.* Unconventional myosins in inner-ear sensory epithelia. *J. Cell Biol.* **137,** 1287–1307 (1997).
14. Buss, F. *et al.* The localization of myosin VI at the Golgi complex and leading edge of fibroblasts and its phosphorylation and recruitment into membrane ruffles of A431 cells after growth factor stimulation. *J. Cell Biol.* **143,** 1535–1545 (1998).
15. Mermall, V., McNally, J. G. & Miller, K. G. Transport of cytoplasmic particles catalysed by an unconventional myosin in living *Drosophila* embryos. *Nature* **369,** 560–562 (1994).
16. Kron, S. J. & Spudich, J. A. Fluorescent actin filaments move on myosin fixed to a glass surface. *Proc. Natl Acad. Sci. USA* **83,** 6272–6276 (1986).
17. Wolenski, J. S., Cheney, R. E., Mooseker, M. S. & Forscher, P. *In vitro* motility of immunoadsorbed brain myosin-V using a *Limulus* acrosomal process and optical tweezer-based assay. *J. Cell Sci.* **108,** 1489–1496 (1995).
18. Jontes, J. D., Wilson-Kubalek, E. M. & Milligan, R. A. A 32 degree tail swing in brush border myosin I on ADP release. *Nature* **378,** 751–753 (1995).
19. Henningsen, U. & Schliwa, M. Reversal in the direction of movement of a molecular motor. *Nature* **389,** 93–96 (1997).
20. Sablin, E. P. *et al.* Direction determination in the minus-end-directed kinesin motor ncd. *Nature* **395,** 813–816 (1998).
21. Endow, S. A. & Waligora, K. W. Determinants of kinesin motor polarity. *Science* **281,** 1200–1202 (1998).
22. Hirose, K., Cross, R. A. & Amos, L. A. Nucleotide-dependent structural changes in dimeric NCD molecules complexed to microtubules. *J. Mol. Biol.* **278,** 389–400 (1998).
23. Sosa, H. *et al.* A model for the microtubule-Ncd motor protein complex obtained by cryo-electron microscopy and image analysis. *Cell* **90,** 217–224 (1997).
24. Sweeney, H. L. *et al.* Kinetic tuning of myosin via a flexible loop adjacent to the nucleotide binding pocket. *J. Biol. Chem.* **273,** 6262–6270 (1998).
25. Hopp, T. P. *et al.* A short polypeptide marker sequence useful for recombinant protein identification and purification. *Biotechnology* **6,** 1205–1210 (1988).
26. Kolodziej, P. A. & Young, R. A. Epitope tagging and protein surveillance. *Methods Enzymol.* **194,** 508–519 (1991).
27. Espreafico, E. M. *et al.* Primary structure and cellular localization of chicken brain myosin-V (p190), an unconventional myosin with calmodulin light chains. *J. Cell Biol.* **119,** 1541–1557 (1992).
28. Pollard, T. D. Assays for myosin. *Methods Enzymol.* **85,** 123–130 (1982).
29. Elzinga, M. & Phelan, J. J. F-actin is intermolecularly crosslinked by N,N′-*p*-phenylenedimaleimide through lysine-191 and cysteine-374. *Proc. Natl Acad. Sci. USA* **81,** 6599–6602 (1984).
30. Jontes, J. D. & Milligan, R. A. Brush border myosin-I structure and ADP-dependent conformational changes revealed by cryoelectron microscopy and image analysis. *J. Cell Biol.* **139,** 683–693 (1997).

Acknowledgements

This work was supported by grants from the NIH. We thank M. S. Mooseker for the chicken myosin V cDNA, and G. Daniels of Leica Microsystems for technical support.

Correspondence and requests for materials should be addressed to H.L.S. (e-mail: Lsweeney@mail.med.upenn.edu).

erratum

Changing spatial structure of the thermohaline circulation in response to atmospheric CO_2 forcing in a climate model

Richard A. Wood, Ann B. Keen, John F. B. Mitchell & Jonathan M. Gregory

Nature **399,** 572–575 (1999)

The scale vectors shown at the bottom left of each panel in Fig. 2 were the wrong size as published; the corrected figure is shown below.□